JOURNAL OF MATERIALS SCIENCE 27 (1992) 5303–5305

Partial phase diagram of new quarternary semiconductor $Pb_{1-x}Mn_xS_{1-y}Se_y$ for mid-infrared lasers

T. KIYOSAWA, S. TAKAHASHI, N. KOGUCHI
National Research Institute for Metals, Tsukuba Laboratories, 1-2-1 Sengen, Tsukuba-shi Ibaraki 305, Japan

The phase diagram of the PbS–PbSe–MnSe–MnS system was investigated with an emphasis on the lead-rich $Pb_{1-x}Mn_xS_{1-y}Se_y$ solid solution by differential thermal analysis, X-ray powder diffraction method and X-ray micro analysis. The T–x phase diagrams of the PbS–MnS and PbSe–MnSe systems are presented. The isothermal phase diagram of the PbS–PbSe–MnSe–MnS system are also presented for $T \leqslant 950\,^{\circ}C$. The solid solubility and lattice constant of the $Pb_{1-x}Mn_xS_{1-y}Se_y$ solid solution were determined.

1. Introduction

Lead chalcogenides containing manganese have been studied as diluted magnetic-semiconducting materials [1]. $Pb_{1-x}Mn_xS$ and $Pb_{1-x}Mn_xSe$ solid solution have been fabricated into p–n homojunction lasers and their mid-infrared emissions have been found to be tuned by a magnetic field [2, 3]. This indicates that the solid solutions are promising materials for use as magnetically tunable diode lasers which are suitable light sources for high-sensitivity spectroscopic systems [4] and for prospective optical-fibre communication systems using extremely low-loss fluoride glass fibres [5].

Application of lattice-matched double-hetero and/or quantum-well structure of laser diodes to the materials is expected to improve the performance of PbS-based laser diodes. This makes the $Pb_{1-x}Mn_xS_{1-y}Se_y$ quarternary alloy a promising material and the knowledge of its phase diagram, lattice constant, band gap energy and refractive index is required.

This paper reports an investigation of the partial phase diagram of the PbS–PbSe–MnSe–MnS system as well as the solid solubility range and lattice constant of the $Pb_{1-x}Mn_xS_{1-y}Se_y$ solid solution.

2. Preparation of materials and measurement techniques

Materials with various compositions in the PbS–PbSe–MnSe–MnS system were prepared from 99.9999% grade lead ingot, sulphur powder and selenium shot and 99.999% grade manganese lump by the standard method of melting and water quenching. To achieve this, several grams of the elemental mixture were sealed in a cleaned quartz ampoule under a vacuum of 10^{-6} torr. (1 torr = 133.322 Pa). After the ampoule was heated carefully with a hand torch to react the elements, it was introduced into a furnace and kept at about 1130 °C for 5 h and subsequently water quenched.

Differential thermal analysis (DTA) was applied to the materials of the PbS–MnS ($y = 0$) and PbSe–MnSe ($y = 1$) systems. The water-quenched bulk materials with various compositions were ground into powders. About 50 mg each powder were sealed under vacuum in a thin-walled quartz ampoule with capacity of around 3 mm diameter × 5 mm. A similar quartz ampoule containing about 30 mg alumina was used as a reference. Pt/Pt–13%Rh thermo-couples detected the sample temperature and the temperature difference between the sample and the reference. Calibration runs were made using silver and gold. Heating and cooling were carried out at a rate of 10 K min^{-1} with several minutes of holding at a temperature lower by 40–70 K than the expected temperature for an endothermic reaction and at a temperature higher by 10–40 K than the expected temperature for an exothermic reaction. The recalescence did not exceed 2 K. The thermal reaction temperatures were obtained by two methods. One was to find an intersection of a base line and a tangent with maximum gradient on a DTA curve at the onset of a thermal reaction (extrapolated start point). The other was to find a deflection point from a linear relation on a plot of log (ΔT) versus time of a DTA curve after a peak of a thermal reaction (end point), where ΔT was the temperature difference between the DTA curve and its base line. The solidus temperature, for example, was determined as the extrapolated start point of the heating DTA curve and as the end point of cooling DTA curve. The temperatures obtained by the two methods differed from each other by 1–9 K and the mean temperature was assigned to the solidus temperature.

X-ray powder diffraction measurement and X-ray microanalysis (XMA) were performed to examine the solid-phase equilibria in the PbS–PbSe–MnSe–MnS system and the lattice parameter of the lead-rich $Pb_{1-x}Mn_xS_{1-y}Se_y$ solid solution. Samples for XMA were prepared by annealing the water-quenched bulk materials at 825 and 723 °C with subsequent water

0022–2461

quenching, and those for X-ray powder diffraction by annealing the ground powder materials at various temperatures between 500 and 950 °C. Care was taken to keep a uniform temperature within the ampoule. The annealing time was varied in order to ensure that an equilibrium state was obtained. Typically, 4 days at a temperature below 700 °C and 1 day for 700 °C and above was sufficient. The lattice constant of the $Pb_{1-x}Mn_xS_{1-y}Se_y$ solid solution, which has the NaCl structure, was calculated from extrapolation of the least-square equation for the spacing versus $\cos^2\theta$ plot for reflections higher than (6 2 0).

3. Results and discussion

3.1. *T–x* phase diagrams of the PbS–MnS and PbSe–MnSe system

The partial *T–x* phase diagrams of the PbS–MnS and the PbSe–MnSe systems are represented in Figs 1 and 2, respectively. The results of DTA are also indicated. The solubility limits of the lead-rich $Pb_{1-x}Mn_xS$ and $Pb_{1-x}Mn_xSe$ solid solution were determined from the change of their lattice constant with manganese content, as exemplified later in Fig. 4. It is seen from Fig. 1 that $Pb_{1-x}Mn_xS$ solid solution has retrograde solubility and coexists with MnS, and that there may be two invariant reactions at 1045 ± 4 and 1024 ± 4 °C. Detail of the reactions has not yet been revealed. The PbSe–MnSe system (Fig. 2) shows retrograde solubility of manganese into PbSe and the coexistence of $Pb_{1-x}Mn_xSe$ solid solution with MnSe, similar to the PbS–MnS system. The reaction at 1016 ± 4 °C is regarded as a eutectic reaction, liq. = $Pb_{1-x}Mn_xSe$ + MnSe.

3.2. Isothermal phase diagram

The isothermal phase diagram at 723 °C of the PbS–PbSe–MnSe–MnS system is shown in Fig. 3. The solubility limits of manganese in the $Pb_{1-x}Mn_xS$ and $Pb_{1-x}Mn_xSe$ solid solution were obtained through lattice constant measurement. There exist two solid phases: one is the $Pb_{1-x}Mn_xS_{1-y}Se_y$ solid solution with the NaCl structure (α) and the other is the $MnS_{1-z}Se_z$ solid solution with the NaCl structure (β) containing a slight amount of lead (< 1%). The isothermal phase diagram at 825 °C was found to be very similar to that at 723 °C except that the former has an increased α phase region.

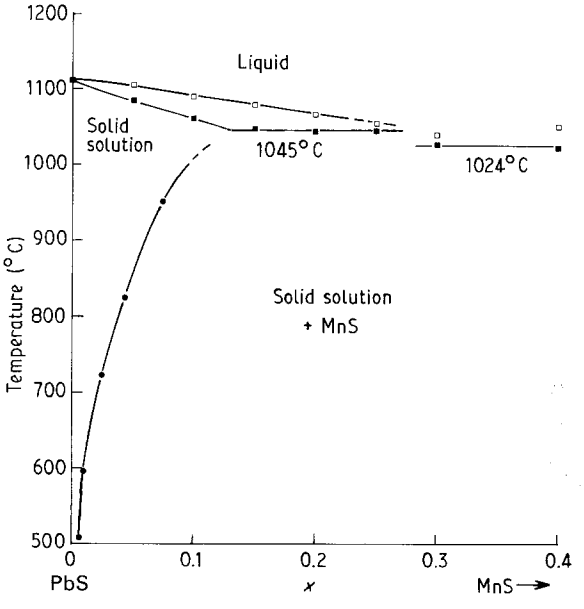

Figure 1 Partial *T–x* phase diagram of the PbS–MnS system. (□, ■) DTA results.

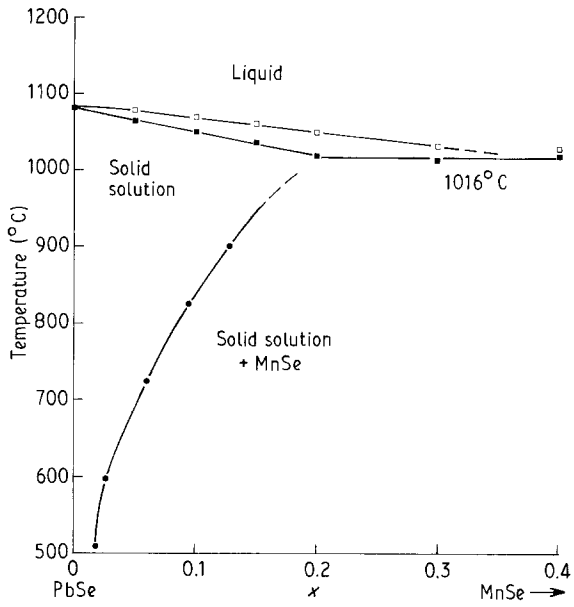

Figure 2 Partial *T–x* phase diagram of the PbSe–MnSe system.

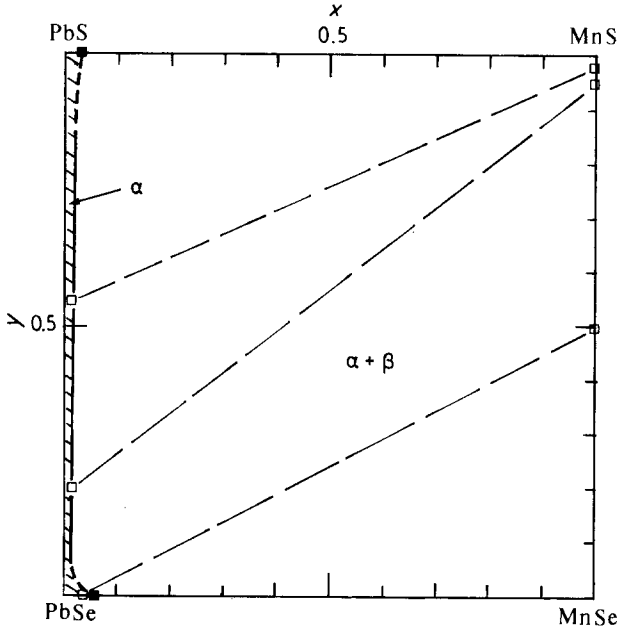

Figure 3 Isothermal phase diagram of the PbS–PbSe–MnSe–MnS system at 723 °C. α, $Pb_{1-x}Mn_xS_{1-y}Se_y$ solid solution; β, $MnS_{1-z}Se_z$ solid function. (□) XMA results; (– – –) the line for compositions of coexisting phases. (■) solubility limits of manganese.

3.3. Lattice constant and existence region of the $Pb_{1-x}Mn_xS_{1-y}Se_y$ solid solution

The variation of the α phase lattice constant with *x* is shown in Fig. 4 for $y = 0$, 0.2, 0.5, 0.8, 0.9 and 1. The

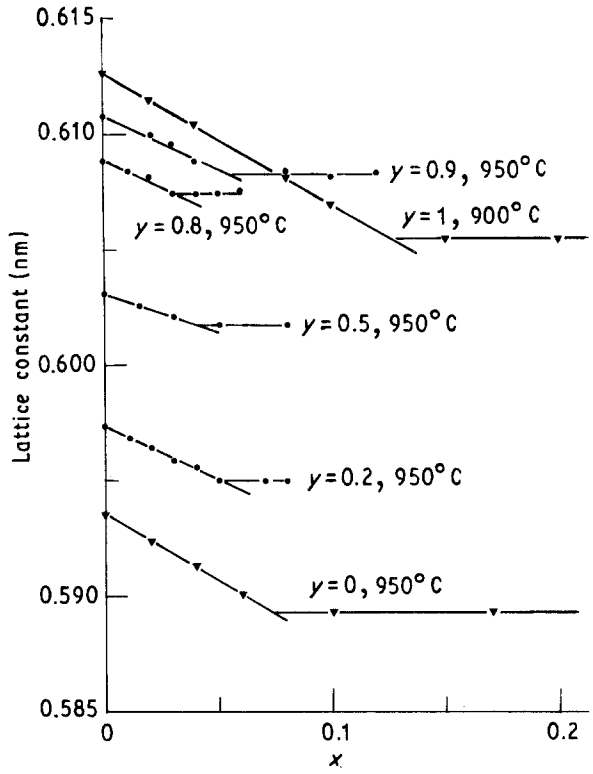

Figure 4 Variation of the lattice constant of the $Pb_{1-x}Mn_xS_{1-y}Se_y$ solid solution with manganese content for $y = 0$, 0.2, 0.5, 0.8, 0.9 and 1.

samples were annealed at 825 or 950 °C, at which the solid solubility limit of manganese was rather large and relations between the lattice constant and x could be deduced. The following relations were obtained

$$a(x) = 0.5936 - 0.058x \text{ (nm)} \quad y = 0 \qquad (1)$$

$$a(x) = 0.5974 - 0.04_7x \text{ (nm)} \quad y = 0.2 \qquad (2)$$

$$a(x) = 0.6031 - 0.03_3x \text{ (nm)} \quad y = 0.5 \qquad (3)$$

$$a(x) = 0.6089 - 0.04_6x \text{ (nm)} \quad y = 0.8 \qquad (4)$$

$$a(x) = 0.6109 - 0.04_6x \text{ (nm)} \quad y = 0.9 \qquad (5)$$

$$a(x) = 0.6127 - 0.057x \text{ (nm)} \quad y = 1 \qquad (6)$$

It is noted that the dependence of the lattice constant on manganese content is similar for $y = 0$ and $y = 1$ but varies with y for $0 < y < 1$, showing a minimum at around $y = 0.5$.

The existence region of the α phase was determined from the results of the lattice constant measurement and XMA, and is shown in Fig. 5 for 950, 825 and 723 °C. It is also noted that the solubility limit of manganese depends strongly on y and reduce sharply with y just parting from $y = 0$ and 1.

4. Conclusion

The phase diagrams presented above could afford a metallurgical basis for preparation of the material.

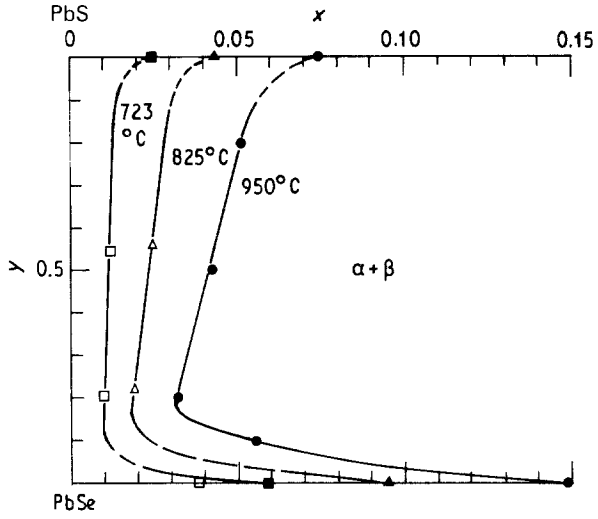

Figure 5 Existence region of the $Pb_{1-x}Mn_xS_{1-y}Se_y$ solid solution at 950, 825 and 723 °C: (●, ▲, ■) from lattice constant measurement, (△, □) from XMA.

Equations 1–6 and Fig. 5 are able to give available compositional conditions for lattice matching within the solid solution region. From this and the results reported previously by us [6] on the compositional dependence of energy gap and refractive index of the solid solution, the $Pb_{1-x}Mn_xS_{1-y}Se_y$ quarternary solid solution is found to be a suitable material for lattice-matched double-heterostructure and/or quantum-well lasers.

Acknowledgements

The authors thank T. Kimura for X-ray micro-analysis, and Dr K. Nii, National Research Institute for Metals and Dr K. Masumoto, The Research Institute of Electric and Magnetic Alloys, for their encouragement.

References

1. J. R. ANDERSON, G. KIDO, Y. NISHINA, M. GORSKA, L. KOWALCZYK and Z. GOLACKI, *Phys. Rev.* **B41** (1990) 1014.
2. G. KARCZEWSKI, L. KOWALCZYK and A. SZCZERBAKOW, *Solid State Commun.* **38** (1981) 499.
3. L. KOWALCZYK and A. SZCZERBAKOW, *Acta Phys. Pol.* **A73** (1988) 447.
4. J. F. BUTLER and J. O. SAMPLE, *Cryogenics* **17** (1977) 661.
5. D. C. TRAN, G. H. SIGEL Jr and B. BENDOW, *J. Lightwave Tech.* **LT-2** (1984) 566.
6. N. KOGUCHI, S. TAKAHASHI and T. KIYOSAWA, *Jpn. J. Appl. Phys.* **27** (1988) L2376.

Received 13 June
and accepted 31 October 1991